Encrypted audio transmission via synchronized chaotic Nd:YAG lasers

L. Cardoza-Avendaño and R.M. López-Gutiérrez
Faculty of Engineering Architecture and Design, Baja California Autonomous University (UABC), Km 103 Carretera Tijuana-Ensenada, Ensenada B.C., México.

C. Cruz-Hernández*, V.V. Spirin and R.A. Chávez-Pérez
Electronics and Telecommunications Department, Scientific Research and Advanced Studies Center of Ensenada (CICESE), Carretera Ensenada-Tijuana No. 3918, Zona Playitas, 22860 Ensenada B.C., México.
**(CICESE), Electronics and Telecommunications Department, P.O. Box 434944, San Diego, CA 92143-4944, USA, Phone: +52.646.1750500, Fax: +52.646.1750554, e-mail: ccruz@cicese.mx.*

A. Arellano-Delgado
Faculty of Engineering Architecture and Design, Baja California Autonomous University (UABC), Km 103 Carretera Tijuana-Ensenada, Ensenada B.C., México.

Recibido el 7 de noviembre de 2011; aceptado el 31 de agosto de 2012

In this paper, encrypted audio transmission via synchronization of coupled chaotic Nd:YAG lasers in master-slave configuration is numerically studied. In particular, we resort to recent results from complex systems theory to achieve chaos synchronization. So that, enconding, transmission, and decoding of confidential audio messeges in chaotic optical communications are presented. In addition, we show transmission of encrypted audio messages when parameter mismatch and channel noise are considered. In order to illustrate this robustness synchronization property, we present the encrypted transmission of audio messages via an improved chaotic transmitted signal, and we obtain at the receiver that, the original audio message is appropriatelly recovered.

Keywords: Chaos synchronization; encryption; private optical communication; chaotic Nd:YAG laser; complex networks.

Se estudia numéricamente la transmisión de mensajes cifrados de audio con base en la sincronizacion de láseres caóticos de Nd:YAG en configuración maestro y esclavo. Para sincronizar los láseres caóticos, apelamos a resultados recientes de la teoría de sincronización de redes complejas. También se presenta el cifrado, transmisión y descifrado de mensajes de audio en comunicaciones ópticas caóticas. Se estudia la transmisión del mensaje de audio cifrado cuando se varian los parámetros y se agrega ruido al canal. Se muestra la sincronización aproximada del láser esclavo apesar de las perturbaciones añadidas al laser maestro. Para ilustrar la robustez en la sincronización, se estudia la transmisión de un mensaje de audio encriptado a través de una portadora caótica más compleja y el receptor recupera eficientemente el audio original.

Descriptores: Sincronización de caos; cifrado; comunicaciones ópticas privadas; láser caótico Nd:YAG; redes complejas.

PACS: 05.45.-a; 05.45.Gg; 05.45.Pq; 05.45.Vx; 05.45.Xt

1. Introduction

Two of the major requirements in modern communication systems are privacy and security. For contribute in this area, chaotic synchronization, see *e.g.* [1-7] and references therein has been greatly motivated by the possibility of encoding information by using a chaotic carrier or, chaotic encryption [8,9]. This possibility was first explored with *electronic oscillator circuits*, see *e.g.* [10-15], where an analog or digital signal (the confidential information) was imbedded into the transmitted chaotic signal by direct modulation, masking or, another technique. If chaotic synchronization is achieved between transmitter and receiver circuits, then at the receiver end it is possible to extract the encrypted information from the transmitted chaotic signal.

Information transmission based on chaotic synchronization of lasers has been studied recently [16-18]. En particular for *solid-state lasers* [19,20] *fibre ring lasers* [19,21] *semiconductor lasers* [19,22-25] and *microchip lasers* [19]. A chaotic laser may generate an irregular sequence of pulses spaced by periods of very high-intensity, this type of carrier is suitable for masking analog data since the information would be separated from this chaotic carrier due to high-intensity periods, with the appropriate receiver only.

Chaotic optical communication is a promising technique to improve both privacy and security in communication networks. It needs chaotic synchronization between transmitter and receiver lasers to encode, transmit, and decode confidential information. The generated chaotic carrier at the transmitter laser is used to encrypt information, which can only be extracted by using the appropriate receiver laser. An alternative way to improve privacy and security of encrypted information, can be realized by additionally encoding at the physical layer by using chaotic carriers generated by com-

ponents operating in chaotic regime. For example, chaotic solid-state Nd:YAG (*Neodymium doped: Yttium Aluminium Garnet*) lasers are ideal candidates for the realization of these chaotic transmitter and receiver systems [19,26]. They are already inherently nonlinear devices that, under certain operating conditions, exhibit chaotic motion. Different authors investigated analytically and numerically various types of synchronous behaviors that occur when chaotic Nd:YAG lasers are coupled [27-29]. Network synchronization of chaotic Nd:YAG lasers in star topology is reported in Ref. 29, where different collective behaviors are imposed. In Ref. 30 robust synchronization of two chaotic Nd:YAG lasers is discussed when parameter mismatch and channel noise are considered, in addition an application to transmit encrypted binary information is given. While in Ref. 31 the same robust synchronization problem for master-slave chaotic Nd:YAG lasers is addressed; in this case, based on nonlinear stability theory, it is shown that the state trajectories of the perturbed error synchronization are ultimately bounded. So that, encoding, transmission, and decoding of binary information in chaotic optical communications are presented.

The aim of this paper is to study the encoding, transmission, and decoding of confidential audio information in chaotic optical communications, when parameter mismatch and channel noise are present. This objective is achieved by appealing to recent results from complex systems theory, see *e.g.* [32,33]. This robustness study is important since the lasers have differences between them in any practical implementation, due to aging of physical components, uncertainties, and other perturbations. We show that the proposed approach is indeed suitable to synchronize chaotic Nd:YAG lasers in master-slave configuration with parameter mismatch and channel noise. In order to illustrate this robustness synchronization property, we present the effects of parameter mismatch and channel noise on the encoding, transmission, and decoding of confidential audio information in optical chaotic communications, and we evaluate the quality of the recovered audio information. This work complements the results reported in Refs. 30 and 31 where parameter mismatch and channel noise are considered in the transmission of encrypted binary information. At the same time, we mention some substantial differences with [30,31]:

- The context we use here is the encrypted audio transmission. This on the one hand makes the presentation even simpler than in digital communications. On the other hand, to the best of our knowledge it has not reported in the literature.
- The proposed chaotic optical communication scheme uses two transmission channels; so, the processes of encryption and synchronization are completely separated with no interference between them.
- In addition, we propose an *improved chaotic optical communication scheme (ICOCS)* to increase the security of the encryption in the transmitted chaotic signal.
- By means of various measurement tools (autocorrelation, frequency spectrum, and chaotic attractors in phase portrait) that are used in chaos theory we make an attempt to show that the transmitted chaotic signal in ICOCS gives a more complex chaotic signal.

This paper is arranged as follows: A brief review on synchronization of complex networks is given in Sec. 2. Whereas, in Sec. 3, the mathematical model of the solid-state Nd:YAG laser used (as fundamental node) in the chaotic encryption scheme is described. In Sec. 4, master-slave synchronization of chaotic Nd:YAG lasers is presented. In Sec. 5, an application to encrypt audio information in optical chaotic communications is given. Furthermore, we illustrate the effects of parameter mismatch and channel noise on the encoding, transmission, and decoding of audio messages in Sec. 6. Finally, in Sec. 7 some concluding remarks are given.

2. Background on synchronization of complex networks

2.1. Complex networks

Firstly, we give a brief review on complex dynamical networks and its synchronization. For details, see *e.g.* [32,33]. Consider a *complex network* composes of N identical nodes, linearly and diffusively coupled through the first state of each node. In this complex network, each node constitutes a n-*dimensional dynamical system*, described as follows

$$\dot{\mathbf{x}}_i = f(\mathbf{x}_i) + u_i, \quad i = 1, 2, \ldots, N, \tag{1}$$

where $\mathbf{x}_i = (x_{i1},\ x_{i2},\ \ldots, x_{in})^T \in \mathbb{R}^n$ are the *state* variables of the node i, $u_i = u_{i1} \in \mathbb{R}$ is the *input* signal of the node i, and is defined by

$$u_{i1} = c\sum_{j=1}^{N} a_{ij}\Gamma\mathbf{x}_j, \quad i = 1, 2, \ldots, N, \tag{2}$$

the constant $c > 0$ represents the *coupling strength* of the complex network, and $\Gamma \in \mathbb{R}^{n\times n}$ is a constant 0-1 matrix linking coupled state variables. For simplicity, assume that $\Gamma = \mathrm{diag}\,(r_1,\ r_2, \ldots, r_n)$ is a diagonal matrix with $r_i = 1$ for a particular i and $r_j = 0$ for $j \neq i$. This means that two coupled nodes are linked through their $i - th$ state variables. Whereas, $\mathbf{A} = (a_{ij}) \in \mathbb{R}^{N\times N}$ is the *coupling matrix*, which represents the coupling topology of the complex network. If there is a connection between node i and node j, then $a_{ij} = 1$; otherwise, $a_{ij} = 0$ for $i \neq j$. The diagonal elements of coupling matrix $\mathbf{A}$ are defined as

$$a_{ii} = -\sum_{j=1,\ j\neq i}^{N} a_{ij} = -\sum_{j=1,\ j\neq i}^{N} a_{ji}, \quad i = 1, 2, \ldots, N. \tag{3}$$

If the *degree* of node i is d_i, then $a_{ii} = -d_i$ for $i = 1, 2, \ldots, N$.

Suppose that the complex network is connected without isolated clusters. Then, $\mathbf{A}$ is a symmetric irreducible matrix. In this case, it can be shown that zero is an eigenvalue of $\mathbf{A}$ with multiplicity 1 and all the other eigenvalues of $\mathbf{A}$ are strictly negative [32,33].

Synchronization state of nodes in complex networks, can be characterized by the nonzero eigenvalues of $\mathbf{A}$. The complex network (1)-(2) is said to achieve (asymptotically) **synchronization**, if [33]:

$$\mathbf{x}_1(t) = \mathbf{x}_2(t) = \ \ldots \ = \mathbf{x}_N(t), \quad \text{as } t \to \infty. \tag{4}$$

The diffusive coupling condition (3) guarantees that the synchronization state is a solution, $\mathbf{s}(t) \in \mathbb{R}^n$, of an isolated node, that is

$$\dot{\mathbf{s}}(t) = f(\mathbf{s}(t)), \tag{5}$$

where $\mathbf{s}(t)$ can be an *equilibrium point*, a *periodic orbit*, or a *chaotic attractor*. Thus, stability of the synchronization state,

$$\mathbf{x}_1(t) = \mathbf{x}_2(t) = \ \ldots \ = \mathbf{x}_N(t) = \mathbf{s}(t), \tag{6}$$

of complex network (1)-(2) is determined by the dynamics of an *isolated* node, *i.e.* -function f and solution $\mathbf{s}(t)$-, the coupling strength c, the inner linking matrix Γ, and the coupling matrix $\mathbf{A}$.

2.2. Synchronization criterion

The following theorem give the conditions to achieve network synchronization as is established in (4).

Theorem [32,33] *Consider the dynamical network (1)-(2). Let*

$$0 = \lambda_1 > \lambda_2 \geq \lambda_3 \geq \cdots \geq \lambda_N \tag{7}$$

be the eigenvalues of its coupling matrix $\mathbf{A}$. *Suppose that there exists* $n \times n$ *diagonal matrix* $\mathbf{D} > 0$ *and two constants* $\bar{d} < 0$ *and* $\tau > 0$, *such that*

$$[Df(\mathbf{s}(t)) + d\Gamma]^T \mathbf{D} + \mathbf{D}\,[Df(\mathbf{s}(t)) + d\Gamma] \leq -\tau \mathbf{I}_n, \tag{8}$$

for all $d \leq \bar{d}$, *where* $\mathbf{I}_n \in \mathbb{R}^{n\times n}$ *is an unit matrix. If, moreover,*

$$c\lambda_2 \leq \bar{d}, \tag{9}$$

then, the synchronization state (6) of dynamical network (1)-(2) is exponentially stable.

Since $\lambda_2 < 0$ and $\bar{d} < 0$, inequality (9) is equivalent to

$$c \geq \left| \frac{\bar{d}}{\lambda_2} \right|. \tag{10}$$

A small value of λ_2 corresponds to a large value of $|\lambda_2|$, which implies that complex network (1)-(2) can synchronize with a small coupling strength c. Therefore, synchronizability of the complex networks (1)-(2) with respect to a particular coupling topology can be characterized by the second largest eigenvalue of $\mathbf{A}$.

2.3. Globally coupled networks

The coupling topologies commonly studied in synchronization of complex networks (1)-(2) are for example: *globally coupled networks*, *nearest-neighbor coupled networks*, and *star coupled networks*. In this work, we consider only complex networks composed of identical nodes globally coupled. The *global coupled topology* means that any two different nodes in complex network (1)-(2) are connected directly. All nodes are connected to the same number of nodes $(N-1)$. So, the corresponding *coupling matrix* $\mathbf{A}$ is given by

$$\mathbf{A} = \begin{bmatrix} 1-N & 1 & 1 & \cdots & 1 \\ 1 & 1-N & 1 & \cdots & 1 \\ \vdots & \ddots & \ddots & \ddots & \vdots \\ 1 & 1 & 1 & \cdots & 1 \\ 1 & 1 & 1 & \cdots & 1-N \end{bmatrix}. \tag{11}$$

This matrix has a single eigenvalue at 0 and all the others equal to $-N$. Hence, the second largest eigenvalue $\lambda_2 = -N$ decreases to $-\infty$ as $N \to \infty$, *i.e.*,

$$\lim_{N\to\infty} \lambda_2 = -\infty. \tag{12}$$

3. Chaotic Nd:YAG laser like nodes

The following differential equations describe the time evolution of the complex, slowly varying electric field E and gain G of a pair of spatially coupled, single transverse and longitudinal mode class B lasers, reported in Refs. 34 and 35, for laser 1:

$$\begin{aligned} \frac{dE_1}{dT} &= \frac{1}{\tau_c}\left(\left(G_1 - \epsilon_1\right)E_1 - \kappa E_2\right) + i\omega_1 E_1, \\ \frac{dG_1}{dT} &= \frac{1}{\tau_f}\left(p_1 - G_1 - G_1\left|E_1\right|^2\right), \end{aligned} \tag{13}$$

and for laser 2

$$\begin{aligned} \frac{dE_2}{dT} &= \frac{1}{\tau_c}\left(\left(G_2 - \epsilon_2\right)E_2 - \kappa E_1\right) + i\omega_2 E_2, \\ \frac{dG_2}{dT} &= \frac{1}{\tau_f}\left(p_2 - G_2 - G_2\left|E_2\right|^2\right), \end{aligned} \tag{14}$$

where τ_c is the cavity round trip time ($\approx$450 ps for a cavity of length of 6 cm), τ_f is the fluorescence time of the upper lasing level of the Nd^{3+} ion (estimated to be 240 μs for the 1064 nm transition), p_1 and p_2 are the pump coefficients, ϵ_1 and ϵ_2 are the cavity loss coefficients, and ω_1 and ω_2 (angular frequencies) are the detunings of the lasers from a common cavity mode. The lasers are coupled mutually (linearly) with strength κ, assumed to be small, and the sign of the coupling terms is chosen to account for the observed stale phase-locked state in which the lasers have a phase difference of 180°. For laser beams of Gaussian intensity profile and $1/e^2$ beam radius r the coupling strength,

as determined from the overlap integral of the two fields, is defined as $\kappa = \exp\left(-d^2/2r^2\right)$. Control parameters are the frequency detuning of the lasers ($\omega_2 - \omega_1$) and the coupling coefficient κ.

If identical laser parameters are considered, except in the case of modulation of their losses and redimensionalize time in unitis of the round trip time of light around the cavity, τ_c, then Eq. (13)-(14) can be rewrite as follows [35], for laser 1:

$$\frac{dX_1}{dt} = (F_1 - (\alpha_0 + \alpha_1 \cos\omega t)) X_1 - \beta X_2 \cos\Phi,$$
$$\frac{dF_1}{dt} = \gamma\left(A_0 - F_1 - F_1 X_1^2\right), \quad (15)$$

and for laser 2

$$\frac{dX_2}{dt} = (F_2 - (\alpha_0 + \alpha_2 \cos\omega t)) X_2 - \beta X_1 \cos\Phi,$$
$$\frac{dF_2}{dt} = \gamma\left(A_0 - F_2 - F_2 X_2^2\right), \quad (16)$$

with

$$\frac{d\Phi}{dT} = \Delta + \beta\left(\frac{X_2}{X_1} + \frac{X_1}{X_2}\right)\sin\Phi. \quad (17)$$

Now, X_1 and X_2 represent the electric field amplitudes, F_1 and F_2 the gains of the lasers 1 and 2, respectively. Φ is the difference in phases of the electric fields, $\phi_2 - \phi_1$. The parameters α_0 and A_0 denote the rates of intra cavity loss and the rescaled pump parameter, respectively. While the parameter γ contitutes the ratio of the timescales of the electric field τ_c and the spontaneous emission lifetime of the laser material τ_f. Δ constitutes a measure of the detuning of the lasers 1 and 2. The coupled lasers are modulated with a depth α_1 for laser 1 and α_2 for laser 2, of the intra cavity loss at a frequency ω. If the beams have Gaussian profile with $1/e^2$ radius r and are separated by a distance d, then the coupling is proportional to the area of overlap between the two lasers, $\beta \sim e^{-d^2/2r^2}$ [34].

The parameter γ is effectively a measure of stiffness of the system and in the numerical simulations, moderate values of $\gamma \sim 0.01, 0.001$ were considered in order to ease the calculation. Some class B laser media, *i.e.* Ti:Al_2O_3 and CO_2 lasers considered in Ref. 36 have values of γ closer to the regime considered than the Nd:YAG lasers considered in Ref. 37, where γ is of order of magnitude 10^{-6}. However, considering longer resonators in the case of the Nd:YAG lasers would mean the value of γ was somewhat higher. In Ref. 35 was shown synchronization for the mutually coupled pair of model lasers (15)-(17) by using different values β and Φ.

Notice that, if $\beta = \Delta = 0$ in Eq. (15)-(17), then we have following pair of isolated lasers 1 and 2, which are not synchronized

$$\dot{X}_i = (F_i - (\alpha_0 + \alpha_i \cos\omega t)) X_i, \quad i = 1, 2,$$
$$\dot{F}_i = \gamma\left(A_0 - F_i - F_i X^2\right), \quad (18)$$

where $\dot{X}_i = dX_i/dt$ and $\dot{F}_i = dF_i/dt$. Equation (18) corresponds to the isolated model also reported in Ref. 26 for a single solid-state Nd:YAG laser with a sinusoidally modulated loss. In this work, we are interesting in synchronizing the pair of isolated Nd:YAG lasers (18), when are unidirectionally coupled (master-slave coupling), according to Sec. 2.

We performed our simulations by using $\gamma = 10^{-2}$ to avoid stiffness problems that arise with smaller values. It is known that for suitable values of α_0 and α_1, the Nd:YAG lasers (18) exhibit *chaotic oscillations*, we select the following set parameters for chaos: $\alpha_0 = 0.9$, $\alpha_1 = 0.2$, $A_0 = 1.2$, and $\gamma = 0.01$. For the particular case where all losses are modulated equally at the rate [26]; $0.9 + 0.2\cos(0.045t)$, the pump parameters were equal to 1.2. The laser is modulated with a depth α_1 relative to its mean losses α_0. In absence of modulation, the Nd:YAG laser is stable and exhibits damped oscillations to their fixed-point values. Figure 1 shows the chaotic attractor generated by the isolated Nd:YAG laser (18). In all simulations, we keep the values $\alpha_0 \in$ [0.5,1.15] and $\alpha_1 \in$ [0.1,0.3] to ensure chaos.

4. Synchronization of two chaotic Nd:YAG lasers

In this section, we present synchronization of a particular "network", composed of two unidirectionally coupled chaotic Nd:YAG lasers (as described by Eq. (18) for two

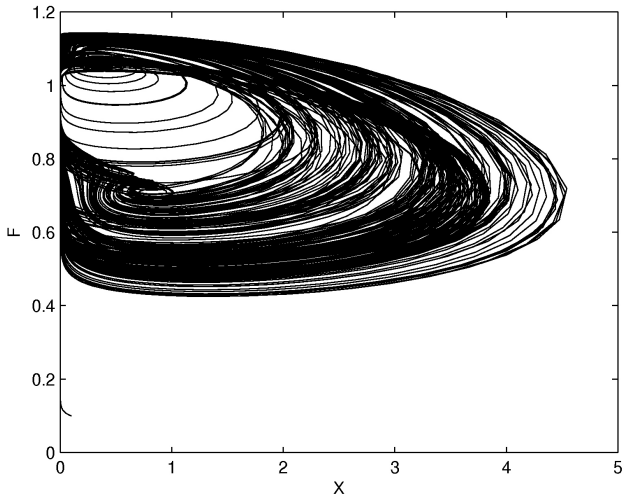

FIGURE 1. Chaotic attractor of Nd:YAG laser.

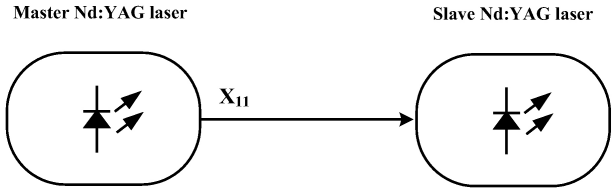

FIGURE 2. Master-slave coupling for chaotic synchronization of two Nd:YAG lasers.

isolated nodes), shown in Fig. 2. Such synchronization is achieved by using the mentioned results from complex networks (Sec. 2); for details, see [30,31]. The master-slave configuration is the laser array, where the coupling is purely via overlap of the electric field [19].

The arrangement of two chaotic Nd:YAG lasers proposed in Refs. 30 and 31, is described by the following state equations, which are based on the chaotic Nd:YAG laser (18) like nodes,

$$\begin{aligned}\dot{X}_{i1} &= \left(F_{i2} - \left(\alpha_0 + \alpha_1 \cos\left(\omega t\right)\right)\right) X_{i1} + u_{i1},\\ \dot{F}_{i2} &= \gamma\left(A_0 - F_{i2} - F_{i2}X_{i1}^2\right), \quad i = 1, 2,\end{aligned} \tag{19}$$

where $X_{i1},\ F_{i2} \in \mathbb{R}^2$ are the state variables of Nd:YAG lasers, $u_{i1} \in \mathbb{R}^2$ is the input signal of the lasers, and is defined by

$$u_{i1} = c\sum_{j=1}^{2} a_{ij} X_{j1}, \quad i = 1, 2, \tag{20}$$

with $c > 0$ the coupling strength of the laser arrays, and $\Gamma \in \mathbb{R}^{2\times 2}$ is a constant 0-1 matrix, $\mathbf{A} = (a_{ij}) \in \mathbb{R}^{2\times 2}$. The diagonal elements of coupling matrix $\mathbf{A}$ are defined as

$$a_{ii} = -\sum_{j=1,\ j\neq i}^{2} a_{ij} = -\sum_{j=1,\ j\neq i}^{2} a_{ji}, \quad i = 1, 2. \tag{21}$$

In this particular coupling topology, the chaotic Nd:YAG laser (*master node*) is defined as

$$\begin{aligned}\dot{X}_{11} &= \left(F_{12} - \left(\alpha_0 + \alpha_1 \cos\left(\omega t\right)\right)\right) X_{11} + u_{11},\\ \dot{F}_{12} &= \gamma\left(A_0 - F_{12} - F_{12}X_{11}^2\right),\end{aligned} \tag{22}$$

with input signal

$$u_{11} = c\left(a_{11}X_{11} + a_{12}X_{21}\right), \tag{23}$$

where $a_{11} = a_{12} = 0$, *i.e.* $u_{11} = 0$.

Whereas, the chaotic Nd:YAG laser (*slave node*) is designed as

$$\begin{aligned}\dot{X}_{21} &= \left(F_{22} - \left(\alpha_0 + \alpha_1 \cos\left(\omega t\right)\right)\right) X_{21} + u_{21},\\ \dot{F}_{22} &= \gamma\left(A_0 - F_{22} - F_{22}X_{21}^2\right),\end{aligned} \tag{24}$$

with input signal

$$u_{21} = c\left(a_{21}X_{11} + a_{22}X_{21}\right), \tag{25}$$

for this case, the coupling matrix (11) is given by

$$\mathbf{A} = \begin{bmatrix} 0 & 0 \\ 1 & -1 \end{bmatrix},$$

the corresponding eigenvalues are $\lambda_1 = -1$ and $\lambda_2 = 0$, with a coupling value $c = 1$ obtained from (10). The numerical results to be presented in next section, were obtained by using a fourth-order Runge-Kutta integration algorithm with step time of size 0.0001. And by taking the initial conditions: $X_{11}(0) = 0.1$, $F_{12}(0) = 0.1$ and $X_{21}(0) = 0.05$, $F_{22}(0) = 0.05$.

In particular, for this network of two coupled chaotic Nd:YAG lasers, we say that the chaotic slave node (24)-(25) asymptotically **synchronizes** with the chaotic master node (22)-(23), if

$$\lim_{t\to\infty} |e_{\mathbf{x}}(t)| = 0 \tag{26}$$

no matter which initial conditions $e_{\mathbf{x}}(0)$ has. Where $e_{\mathbf{x}}(t) = X_{11}(t) - X_{21}(t)$ corresponds to *synchronization error*.

5. Application to encoding, transmission, and decoding

Synchronization of two chaotic Nd:YAG lasers allows us to design private/secure optical communication schemes, where confidential information is encrypted into the transmitter dynamics via chaotic additive masking, chaotic switching, chaotic parameter modulation or, another technique. The master and slave chaotic Nd:YAG lasers are located into the transmitter and receiver systems, respectively. The transmitted chaotic signal through a public channel is a combination of the confidential information with the chaotic output signal of laser transmitter. In particular, encoding, transmission, and decoding of audio messages by using synchronized chaotic Nd:YAG lasers, will be shown in next subsections.

5.1. Encrypted audio transmission

The confidential information is an *audio message* $m(t)$, which is encrypted and transmitted through a public channel. The inclusion of the slave laser is justified when we need to synchronize with the master laser. That is, this process is essential to retrieve information at the receiver end. This communication scheme uses a single transmission channel, but it is well known, that the information recovery is only approximate, due to the processes of synchronization and encryption by the same channel interfere. On the other hand, if we want an exact information recovery at the receiver end, then we can use a communication scheme with two transmission channels. In this case, the slave laser is not necessary for use in the receiver. In order to recovery (exactly) the encrypted information, it is sufficient to subtract chaotic signal and signal chaotic with information. In the sequel, due to space limitations, we show only the results for encrypted transmission with two channels.

Figure 3 shows the scheme for encrypted audio transmission which use the master chaotic Nd:YAG laser (22)-(23) and the slave chaotic Nd:YAG laser (24)-(25) for T and R, respectively. This *chaotic optical communication scheme (COCS)* uses two transmission channels, the first one synchronizes T and R via $X_{11}(t)$. While, the second channel is used to encrypt the confidential audio message $m(t)$: The chaotic signal $X_{11}(t)$ is added to $m(t)$ scaled by $a = 0.01$,

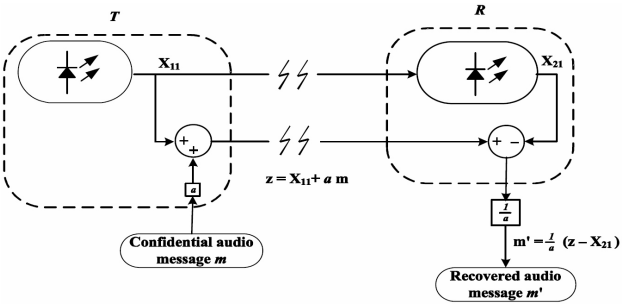

FIGURE 3. Scheme for encryption, transmission, and recovery of audio messages.

such that the negative part of the audio message is encrypted in the transmitted chaotic signal $z(t)$, as follows

$$z(t) = X_{11}(t) + a \cdot m(t). \tag{27}$$

At the receiver end R, to the received chaotic signal $z(t)$ with encrypted audio message, is subtracted the signal $X_{21}(t)$, such that the original audio message $m(t)$ is recovered as $m'(t)$, as follows

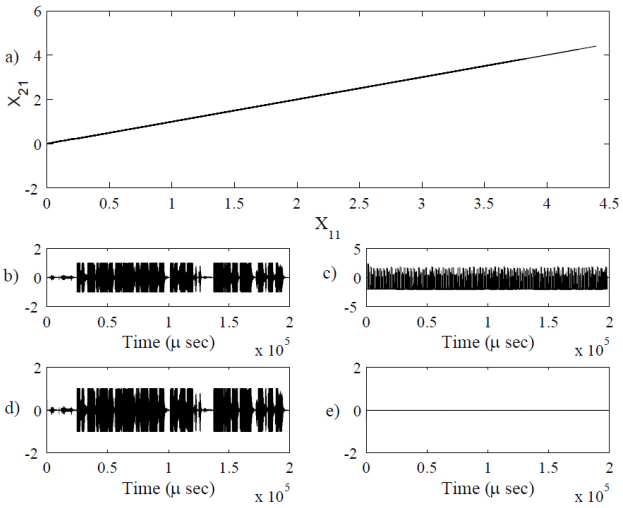

FIGURE 4. Encryption, transmission, and recovery of an audio message: a) chaotic synchronization between X_{11} and X_{21}, b) original audio message $m(t)$, c) transmitted chaotic signal $z(t)$, d) recovered audio message $m'(t)$, and e) signal error $em(t)$ between original and recovered audio messages.

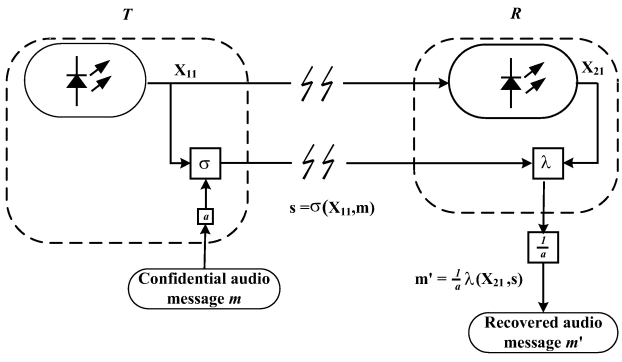

FIGURE 5. Improved scheme for encryption, transmission, and recovery of audio messages by using additional encryption function σ.

$$m'(t) = \frac{1}{a}\left(z(t) - X_{21}(t)\right). \tag{28}$$

The confidential audio message in Spanish: *"Cuerpo Académico Sistemas Complejos y sus Aplicaciones"* is encrypted and transmitted for this demonstration. Figure 4 shows the encryption, transmission, and recovery of the mentioned audio message ("phonogram"): a) chaotic synchronization between X_{11} and X_{21}, b) original audio message $m(t)$, c) transmitted chaotic signal $z(t)$ with encrypted $m(t)$, d) at the receiver end R, the recovered audio message $m'(t)$, and e) the signal error $em(t)$ between the original and recovered audio messages.

Remark. *In COCS, the processes of encryption and synchronization are completely separated with no interference between them. So, the encrypted message does not interfere with synchronization, therefore not increasing the sensitivity of synchronization to external errors. As a result* $m'(t) = m(t)$, *and the chaotic cryptosystem with two transmission channels gives faster synchronization and high security, see* [39,40].

5.2. Improving encrypted audio transmission by using an additional encryption function

We can improve the security of the encrypted audio transmission by using an additional nonlinear encryption function as proposed in Ref. 40. Figure 5 shows the *improved chaotic optical communication scheme (ICOCS)*, where the confidential information $m(t)$ is hidden into transmitted chaotic signal $s(t)$ which is the output signal of nonlinear encryption function

$$\sigma(X_{11}, m) = X_{11}^3 + \left(1 + X_{11}^3\right) a \cdot m. \tag{29}$$

The transmitted chaotic signal $s(t) = \sigma(X_{11}, m)$ is received at the receiver end R. The nonlinear function for decryption is given by

$$\lambda(X_{21}, s) = \frac{-X_{21}^3}{1 + X_{21}^3} + \frac{s}{1 + X_{21}^3}, \tag{30}$$

with chaotic signal $X_{21}(t)$ generated by R, the recovered audio is given by $m'(t) = \frac{1}{a}\lambda\left(X_{21}, s\right)$.

Figure 6 shows the encryption, transmission, and recovery of the same audio message ("phonogram") $m(t)$ with additional encryption function σ: a) chaotic synchronization between X_{11} and X_{21}, b) original audio message $m(t)$, c) transmitted chaotic signal $s(t)$, d) at the receiver end R, the recovered audio message $m'(t)$, and e) the signal error $em(t)$ between $m(t)$ and $m'(t)$.

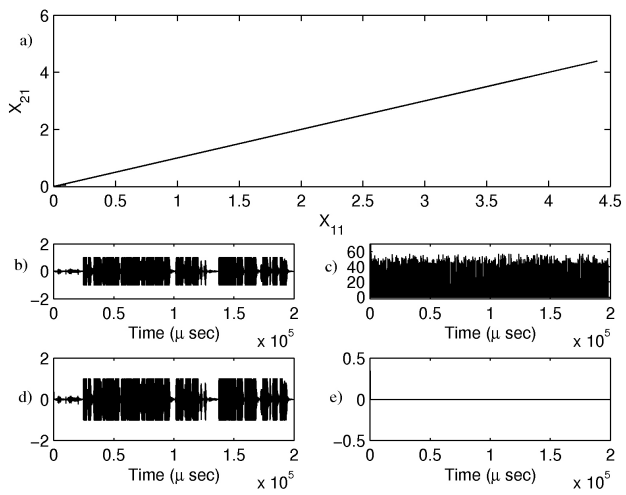

FIGURE 6. Encryption, transmission, and recovery of an audio message by using the improved scheme: a) chaotic synchronization between X_{11} and X_{21}, b) original audio message $m(t)$, c) transmitted chaotic signal $s(t)$, d) recovered audio message $m'(t)$, and e) signal error $em(t)$ between original and recovered audio messages.

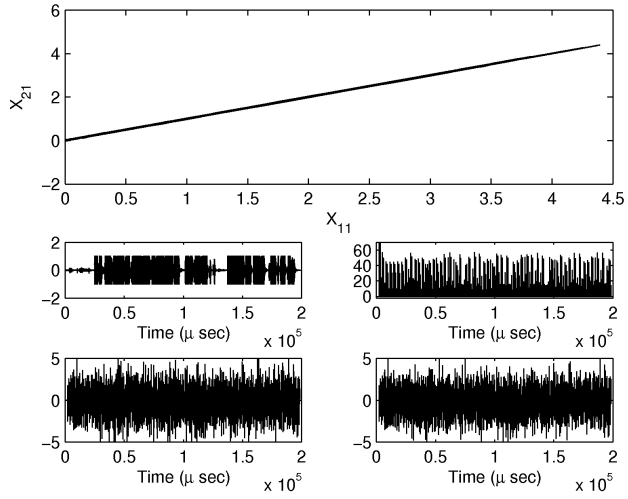

FIGURE 8. Effect of the variation simultaneous in all parameters with channel noise: Audio message transmission: a) chaotic synchronization between X_{11} and X_{21}, b) original audio message $m(t)$, c) transmitted chaotic signal $s(t)$, d) recovered audio message $m'(t)$, and e) signal error $em(t)$ between original and recovered audio messages.

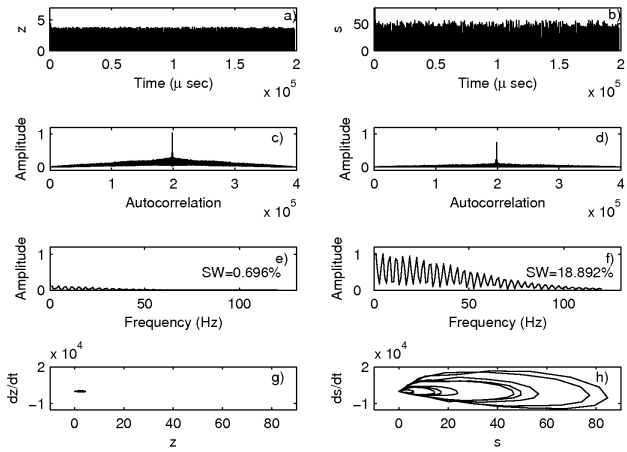

FIGURE 7. Comparison between the transmitted signals $z(t)$ and $s(t)$: a) temporal chaotic signal $z(t)$, b) temporal improved chaotic signal $s(t)$, c) autocorrelation of $z(t)$, d) autocorrelation of $s(t)$, e) frequency spectrum of $z(t)$, f) frequency spectrum of $s(t)$, g) phase-portrait $z(t)$ vs $\dot{z}(t)$, and h) phase-portrait $s(t)$ vs $\dot{s}(t)$.

In the sequel, we make a comparative analysis for both transmitted chaotic signals $s(t)$ and $z(t)$ by using some measurement tools that are used in chaos theory to show that the transmitted chaotic $s(t)$ generates by ICOCS is more complex that $z(t)$; therefore, it is more convenient its usage in chaotic optical communications.

Figure 7 illustrates the transmitted temporal chaotic signals: a) $z(t)$ and b) $s(t)$ generate by COCS and ICOCS, respectively. Firstly, we can see that $s(t)$ has greater amplitude that $z(t)$ and appears to more complex. In order to demonstrate this affirmation, we compare the transmitted chaotic signals $z(t)$ and $s(t)$ through the autocorrelation, frequency spectrum, and phase portrait. Figure 7 shows the results of the comparison between the signals $z(t)$ and $s(t)$; Fig. 7c) shows the autocorrelation of signal $z(t)$ and Fig. 7d) the autocorrelation of signal $s(t)$, notice that the autocorrelation of $s(t)$ is smaller than for the case of $z(t)$, therefore the dynamics of $s(t)$ are richer. For frequency spectrum, here we will evaluate quantitatively the dynamics of $z(t)$ and $s(t)$ by calculating the spectral wealth (SW). Figure 7e) shows the frequency spectrum of $z(t)$ with $SW = 0.696\%$ and Fig. 7f) the frequency spectrum of $s(t)$ with $SW = 18.892\%$; the signal $s(t)$ has greater SW than $z(t)$ indicating that the dynamics of $s(t)$ are richer. Finally, the comparison between $z(t)$ and $s(t)$ is given in phase space, by plotting the signals $z(t)$ versus $\dot{z}(t)$ and $s(t)$ versus $\dot{s}(t)$, called chaotic attractors as was done in Ref. 38. Figure 7g) depicts the chaotic attractor from $z(t)$ and Fig. 7h) the chaotic attractor from $s(t)$. In this case, we can see for $s(t)$ corresponds to an attractor with larger area in phase space in comparison with the attractor for $z(t)$. Indicating again that the dynamics of $s(t)$ are richer.

From this comparative analysis between the transmitted chaotic signals $z(t)$ and $s(t)$, we can say that by adding the encryption function σ to COCS, the transmitted chaotic signal resulting $s(t)$ is a more complex signal, *i.e.* the signal $s(t)$ is more "chaotic" than signal $z(t)$; as a result, we will have greater security in the encrypted audio transmission with ICOCS. Of course, a complete analysis on the security of the encrypted audio transmission with ICOCS is necessary, but will be given in elsewhere.

6. Encrypted audio transmission based on robust synchronization of chaotic Nd:YAG lasers

Finally, we show that synchronization of chaotic Nd:YAG lasers is *robust* with respect to variations in parameters of

master and slave chaotic Nd:YAG lasers, and to additive channel noise. When there are some variations in the parameter values of master and slave Nd:YAG lasers (and/or channel noise), the synchronization is only approximate. That is, the slave Nd:YAG laser (24)-(25) achieves *approximate synchronization* of level ρ with the master Nd:Yag laser (22)-(23), if there exists a constant $\tau > 0$, such that

$$|e_{\mathbf{x}}(t)| \leq \rho, \quad \forall\, t \geq \tau, \tag{31}$$

where $\rho > 0$ is a constant of the synchronization error $e(t) = X_{11}(t) - X_{21}(t)$ and τ is the approximate *synchronization time* [2].

We evaluate the encrypted transmission performance when the parameter values were altered, and determine the intervals of variation where is possible still to recover the confidential audio information $m(t)$. Moreover, we show the effects of the additive channel noise on the information recovery. The analysis of robustness is important since the lasers have differences between them, one can not find two identical lasers that have exactly the same intrinsic parameters, and the presence of noise in the transmission channel. Therefore, to ensure the robustness of optical chaotic communication system (ICOCS) previously presented, the performance of audio recovery for different levels of parameter mismatch between T and R, and noise in the channel is presented. *W* e illustrate the effects of parameter mismatch and channel noise simultaneously on the encoding, transmission, and decoding of the audio message in ICOCS, it is shown in Fig. 8: a) chaotic synchronization between X_{11} and X_{21}, b) the original audio message $m(t)$, c) the transmitted chaotic signal $s(t)$, d) the recovered audio message $m'(t)$, and e) $em(t)$ the signal error between $m(t)$ and $m'(t)$. From this figure we can appreciate that the original audio message is recovered satisfactorily with the variation of each parameter (α_0, α_1, γ, A_0) 10% from the original value, and when the signal-to-noise ratio (SNR) considered is 20.26 dB.

7. Conclusions

In this paper, based on robust chaotic synchronization of Nd:YAG lasers, we have proposed a chaotic optical communication scheme (ICOCS) to encode, transmit, and decode audio confidential messages, when parameter mismatch and channel noise are present. The ICOCS was obtained by adding a nonlinear encryption function as reported in Ref. 40; as a result, we have achieved a transmitted chaotic signal more complex.

We have invoked recent results from complex systems theory to achieved chaos synchronization of Nd:YAG lasers. Thanks to this robust synchronization property, the encrypted transmission and recovery of audio messages were successful.

The significance of this study is because the lasers in practical implementation are different, due to aging of physical components, uncertainties, and other perturbations. So, this work has been shown that the proposed ICOCS is robust and show a great potential for actual optical communication systems in which the encoding is required to be secure. Of course, a complete analysis on the security of the encrypted audio transmission for ICOCS is necessary, but will be given in elsewhere.

Acknowledgments

This work was supported by the CONACYT, México under Research Grant Nos. 166654 and 166039, and by the UABC, México under Research Grant No. 474.

1. L.M. Pecora and T.L. Carroll, *Phys. Rev. Lett*. **64** (1990) 821.
2. C. Cruz-Hernández and A.A. Martynyuk, *Advances in chaotic dynamics with applications*, Vol. 4 (Cambridge Scientific Publishers Ltd., 2010).
3. C. Cruz-Hernández and H. Nijmeijer, *Int. J. Bifurc. Chaos* **10** (2000) 763.
4. H. Sira-Ramírez and C. Cruz-Hernández, *Int. J. Bifurc. Chaos* **11** (2001) 1381.
5. D. López-Mancilla and C. Cruz-Hernández, *Nonlinear Dyn. Syst. Theory* **5** (2005) 141.
6. U. Feldmann, M. Hasler and W. Schwarz, *Int. J. Circ. Theory Appl*. **24** (1996) 551.
7. H. Nijmeijer and I.M.Y. Mareels, *IEEE Trans. Circ. Syst. I* **44** (1997) 882.
8. A.N. Pisarchik and M. Zanin, *Physica D* **237** (2008) 2638.
9. A. Kanso, M. Ghebleh, *Commun Nonlinear Sci Numer Simulat* **17** (2012) 2943.
10. K.M. Cuomo and AV. Oppenheim, *Phys. Rev. Lett.* **71** (1993) 65.
11. H. Dedieu, M.P. Kennedy and M. Hasler, *IEEE Trans. Circ. Syst. II* **40** (1993) 634.
12. D. López-Mancilla and C. Cruz-Hernández, *Revista Mexicana de Física* **51** (2005) 265.
13. C. Cruz-Hernández, D. López-Mancilla, V. García, H. Serrano and R. Núñez, *J. Circ. Syst. Comput*. **14** (2005) 453.
14. L. Gámez-Guzmán, C. Cruz-Hernández, R.M. López-Gutiérrez and E.E. García-Guerrero, *Revista Mexicana de Física* **54** (2008) 299.
15. C. Cruz-Hernández, *Nonlinear Dyn. Syst. Theory* **4** (2004) 1.
16. A. Jacobo, M. C. Soriano, C. R. Miraso, P. Colet, *EEE J. Quant. Electron.* **46** (2010) 499.
17. V.Z. Tronciu, I.V. Ermakov, P. Colet, C. R. Mirasso, *Optics Communications* **281** (2008) 4747.

18. M.W. Lee, P. Rees, .A. Shore, S. Ortin, L. Pesquera, A.Valle, *IEE Proc-Optoelectron.* **152** (2005) 97.
19. A. Uchida, *Optical communication with chaotic lasers*, (Wiley-VCH, 2012).
20. P. Colet and R. Roy, *Opt. Lett*. **19** (1994) 2056.
21. G.D. Van Wiggeren and R. Roy, *Science*, **279** (1998) 1198.
22. C.R. Mirasso, P. Colet and P. García-Fernández, *Phot. Tech. Lett.* **8** (1996) 99.
23. A. Sánchez-Díaz, C. Mirasso, P. Colet and P. García-Fernández, *IEEE J. Quant. Electron*. **35** (1999) 292.
24. K.E., Chlouverakis, A. Argyris, A. Bogris, D. Syvridis, *Physica D* **237** (2008) 568.
25. S. Banerjee, L. Rondoni, S. Mukhopadhyay, *Optics Communication* **284** (2011) 4623.
26. J.R. Terry, *Int. J. Bifurc. Chaos* **12** (2002) 495.
27. P. Ashwin, J.R. Terry, K.S. Thornburg and R. Roy, *Phys. Rev. E* **58** (1998) 7186.
28. J.R. Terry, K.S Thornburg, J.D. DeShazer, D. Van Wiggeren, S. Zhu, P. Ashwin and R. Roy, *Phys. Rev. E* **59** (1999) 4036.
29. Posadas-Castillo C., Cruz-Hernández C., R.M. López-Gutiérrez, *Synchronization in a network of chaotic solid-state Nd:YAG laser.* (Procs of the 17th World Congress, IFAC, Seoul, Korea, July 6-11, 2008).
30. C. Posadas-Castillo, R.M. López-Gutiérrez, C. Cruz-Hernández, *Commun. Nonlinear Sci. Numer. Simulat.*, **13** (2008) 1655.
31. R.M. López-Gutiérrez, C. Posadas-Castillo, D. López-Mancilla and C. Cruz-Hernández, *Chaos, Solitons & Fractals* **42** (2009) 277.
32. X.F. Wang and G. Chen, *Int. J. Bifurc. Chaos* **12** (2002) 187.
33. X.F. Wang, *Int. J. Bifurc. Chaos* **12** (2002) 885.
34. L. Fabiny, P. Colet, R. Roy, and D. Lenstra, *Phys Rev A* **47** (1993) 4287.
35. J. R. Terry, *J. Opt. B: Quantum Semiclass. Opt.* **1** (1999) 245.
36. D. Dangoisse, P. Glorieux, and D. Hennequin, *Phys. Rev. A* **36** (1987) 4775.
37. K. S. Thornburg, Jr., M. Möller, R. Roy, T. W. Carr, R.-D. Li, and T. Erneux, *Phys Rev E* **55** (1997) 3865.
38. L. Cardoza-Avendaño, V.V. Spirin, R.M. López-Gutiérrez, C.A. López-Mercado and C. Cruz-Hernández, *Optical & Laser Technology* **43** (2011) 949.
39. J.A. Zhong-Ping , *IEEE Trans. Circ. Syst. I* **49** (2002) 92.
40. A.Y. Aguilar-Bustos, C. Cruz-Hernández, R.M. López-Gutiérrez and C. Posadas-Castillo, *Nonlinear Dyn. Syst. Theory* **8** (2008) 221.